Structural and functional studies on Ycf12 (Psb30) and PsbZ deletion mutants from a thermophilic cyanobacterium

Kenji Takasaka[a], Masako Iwai[b], Yasufumi Umena[c], Keisuke Kawakami[a], Yukari Ohmori[a], Masahiko Ikeuchi[d], Yuichiro Takahashi[a], Nobuo Kamiya[c], Jian-Ren Shen[a, *]

[a]Division of Bioscience, Graduate School of Natural Science and Technology/Faculty of Science; Okayama University, Okayama 700-8530; [b]Department of Applied Biological Science, Faculty of Science and Technology, Tokyo University of Science, Yamasaki, Noda, Chiba 278-8510; [c]Department of Chemistry, Graduate School of Science, Osaka City University, 3-3-138 Sugimoto, Sumiyoshi, Osaka 558-8585, Japan; [d]Department of Life Sciences (Biology), Graduate School of Arts and Science, The University of Tokyo, Komaba, Meguro, Tokyo 153-8902,

[*]Corresponding author:
Jian-Ren Shen
Division of Bioscience, Graduate School of Natural Science and Technology/Faculty of Science; Okayama University, Okayama 700-8530, Japan. Fax: +81 86 251 8502
E-mail: shen@cc.okayama-u.ac.jp

Keywords: Photosystem II; Mutants; Crystal structure; Ycf12; PsbZ; Oxygen evolution.

Abbreviations: Chl, chlorophyll; DDM, n-dodecyl-β-D-maltoside; hrCNE, high resolution clear native electrophoresis; LDAO, lauryldimethylamine N-oxide; LHCII, light-harvesting complex II; LMW, low molecular weight; NCS, non-crystallographic symmetry; Mes, 4-morpholineethanesulfonic acid; PEG, polyethylene glycol; PSI, photosystem I; PSII, photosystem II; SDS-PAGE, sodium dodecyl sulfate-polyacrylamide gel electrophoresis.

Abstract

Ycf12 (Psb30) and PsbZ are two low-molecular weight subunits of photosystem II (PSII), with one and two trans-membrane helices, respectively. In order to study the functions of these two subunits from a structural point of view, we constructed deletion mutants lacking either Ycf12 or PsbZ from *Thermosynechococcus elongatus*, and purified, crystallized and analyzed the structure of PSII dimer from the two mutants. Our results showed that Ycf12 is located in the periphery of PSII, close to PsbK, PsbZ and PsbJ, and corresponded to the unassigned helix X1 reported previously, in agreement with the recent structure at 2.9 Å resolution (A. Guskov, J. Kern, A. Gabdulkhakov, M. Broser, A. Zouni, W. Saenger, Cyanobacterial photosystem II at 2.9 Å resolution: role of quinones, lipids, channels and chloride, Nat. Struct. Mol. Biol. 16 (2009) 334－342). On the other hand, crystals of PsbZ-deleted PSII showed a remarkably different unit cell constants from those of wild-type PSII, indicating a role of PsbZ in the interactions between PSII dimers within the crystal. This is the first example for a different arrangement of PSII dimers within the cyanobacterial PSII crystals. PSII dimers had a lower oxygen-evolving activity from both mutants than that from the wild type. In consistent with this, the relative content of PSII in the thylakoid membranes was lower in the two mutants than that in the wild type. These results suggested that deletion of both subunits affected the PSII activity, thereby destabilized PSII, leading to a decrease in the PSII content in vivo. While PsbZ was present in PSII purified from the Ycf12-deletion mutant, Ycf12 was present in crude PSII but absent in the finally purified PSII from the PsbZ-deletion mutant, indicating a preferential, stabilizing role of PsbZ for the binding of Ycf12 to PSII. These results were discussed in terms of the PSII crystal structure currently available.

1. Introduction

Photosystem II (PSII) catalyzes light-driven oxidation of water, leading to the evolution of molecular oxygen, which forms and continues to maintain the current oxidative atmosphere. In cyanobacteria, this complex consists of 17 membrane-spanning subunits, three extrinsic proteins, and more than 70 cofactors including chlorophylls (Chls), carotenoids, plastoquinones, pheophytins, manganese atoms, non-heme iron, calcium, chlorides, and heme groups, with a total molecular weight of around 350 kDa for a monomer. Among the 17 trans-membrane subunits, 13 have molecular weight lower than 10 kDa, and are termed low molecular weight (LMW) subunits. Twelve LMW subunits have single trans-membrane helix, and only PsbZ has two trans-membrane helices. The functions of most LMW subunits remain obscure at present.

The crystal structure of PSII has been reported at 3.8-3.0 Å resolutions by X-ray crystallography from two thermophilic cyanobacteria, *Thermosynechococcus elongatus* [1-3] and *T. vulcanus* [4]. In the structure reported at 3.0 Å resolution previously [3], there were three trans-membrane helices whose identities were not determined, and were thus designated X-1, X-2, X-3. Very recently, the resolution of the PSII structure was raised to 2.9 Å, leading to the identification of all PSII subunits, and additional lipids, plastoquinone, etc [5]. In this structure, the three trans-membrane helices X-1, X-2, X-3 were assigned to Ycf12 (Psb30), PsbY, and PsbX, respectively. The assignment of X-2 to PsbY is in agreement with our previous assignment based on the structural analysis of PSII from a PsbY-deletion mutant [6].

Ycf12 is a recently identified LMW subunit of PSII with a molecular weight of ~5.0 kDa [7-9]. The gene encoding this subunit is widely conserved in cyanobacterial genomes and chloroplast genomes of many eukaryophyta including eukaryotic alga and some gymnosperms whose plastid sequences are available, but is not found in the chloroplast and nuclear genomes of angiosperms [10]. In the recent structure [5], Ycf12 was found to be located in the periphery of PSII adjacent to PsbZ, PsbK, and PsbJ. The function of Ycf12 in PSII is not clear at present.

PsbZ is another LMW subunit of PSII and is located close to Ycf12, PsbK and CP43. It is encoded by a gene conserved from cyanobacteria to higher plants, has a molecular weight of around 6.6 kDa, and has been detected in PSII core complexes purified from cyanobacteria [11, 12], a green alga *Chlamydomonoas reinhardtii* [13], and tobacco. PsbZ is the only LMW subunit that has two trans-membrane helices. The function of PsbZ has been studied by mutagenesis from cyanobacteria to higher plants. In a

cyanobacterium *Synechocystis* sp. PCC6803, deletion of PsbZ was found to retard the growth under low light conditions [14], which was taken as evidence to support a function of PsbZ in regulating electron transfer activities through the two photosystems. This is in agreement with results obtained from a tobacco mutant lacking PsbZ, where it was shown that lack of PsbZ resulted in a faster flow of electrons to PSI without a significant effect on the maximum electron transfer capacity of PSII [15]. In green alga and higher plants, depletion of PsbZ was shown to destabilize the PSII-LHCII (light-harvesting complex II) super-complex [13, 16], suggesting the involvement of PsbZ in the interaction between PSII and LHCII. More recently, deletion of PsbZ was shown to lead to the loss of Ycf12 and a significant decrease of PsbK in PSII purified from a thermophilic cyanobacterium *T. elongatus* [9].

In order to elucidate the function of Ycf12 and PsbZ in PSII from a structural point of view, we set out to analyze the PSII structure from mutants lacking Ycf12 or PsbZ from a thermophilic cyanobacterium *T. elongatus*, concomitant with functional analysis of mutant PSII. Our results confirmed the location of Ycf12 assigned in the recent structure reported at 2.9 Å resolution, and revealed that PSII is destabilized in both mutants lacking Ycf12 or PsbZ. Furthermore, we showed that while Ycf12 is not required for the binding of PsbZ to PSII, PsbZ is required for the stable association of Ycf12 to PSII.

2. Materials and methods

2.1. Construction of mutant strains and purification of PSII

T. elongatus cells were grown at 45-49°C with bubbling of air containing 5% CO_2, as described previously [17]. The DNA fragments upstream and downstream of *tsr1242* (*ycf12*) were amplified by PCR with oligonucleotide primers, 5'-CCCTGCAGAGTCTCAGTCCCTAC-3' and 5'-CGGATATCAGTTCGTGATTTTATTT-3', and 5'-AGGATATCGCGGCAATTTGTAGGC-3' and 5'-GCGCGGCCGCCTGCGGGCCTTTGCCC-3', respectively. The 972 bp and 984 bp PCR products were cloned into a plasmid pPCR-Script Amp SK (+) (Stratagene, La Jolla, CA), separately. Following DNA sequencing, the 1.0 kb *Pst*I-*Eco*RV fragment of the upstream and a blunt end fragment of 1.3 kb chloramphenicol-resistant cassette were ligated to the *Not*I-*Eco*RV site of PCR-cloned downstream fragment of *ycf12*. The whole gene of *ycf12* consisting of 141 bp in the cyanobacterium was deleted by natural transformation with this double-crossover recombination construct, as described

previously [17]. The *ycf12*-deletion mutant was segregated and maintained in the presence of 5 μg/ml chloramphenicol, and the deletion of the open-reading frame was confirmed by PCR (data not shown). For large scale purification, the cells were grown in a 50 L liquid culture for 8-12 days in the absence of chloramphenicol. The mutant strain lacking the *psbZ* gene was constructed as described in [9], and cultured similarly as the *ycf12*-deletion mutant.

PSII dimers were purified from *ycf12*- and *psbZ*-deletion mutants according to Shen and Inoue [18, 19] with slight modifications. Crude-PSII was obtained by treatment of thylakoids with lauryldimethylamine N-oxide (LDAO), which was then solubilized by 1.0% (w/v) n-dodecyl-β-D-maltoside (DDM) and loaded onto a TOYOPEARL DEAE 650M (Tosoh Co.) column equilibrated with a solution of 30 mM Mes (pH 6.0), 0.03% DDM. The column was washed with 90 mM NaCl to remove phycobili-proteins and PSI complexes, and the PSII-containing fraction was eluted with 125 mM NaCl. The PSII fraction was precipitated in the presence of 12% polyethylene glycol (PEG) 1,450, re-solubilized with 0.6% DDM, and then purified by a second column Q-sepharose High Performance (GE Healthcare UK Ltd.) with a gradient of 200-300 mM NaCl. The PSII dimer fractions from the column was collected, precipitated by centrifugation after addition of 12% PEG 1450, and used for crystallization as well as functional analysis. In some cases, PSII were purified from the *ycf12*-deletion mutant by the single column of Q-sepharose High Performance, which yielded PSII dimers with enough purity.

2.2. Electrophoresis and gel filtration chromatography

Sodium dodecyl sulfate-polyacrylamide gel electrophoresis (SDS-PAGE) was carried out with a 16%-22% polyacrylamide gradient gel containing 7.5 M urea at room temperature [20]. Samples were solubilized with 2% lithium dodecyl sulfate, 60 mM dithiothreitol and 60 mM Tris-HCl (pH 8.5), and incubated for 10 min on ice.

For analysis of the amount of PSI trimer, PSII dimer and PSII monomer in thylakoids, high resolution Clear Native Electrophoresis (hrCNE) was performed according to [21, 22], with slight modifications. Thylakoids were suspended in a suspending buffer containing 25% glycerol, 50 mM imidazole (pH 7.0), 120 mM 6-amino hexanoic acid, 10 mM $MgCl_2$ to a chlorophyll (Chl) concentration of 90 μg Chl/ml, and centrifuged for 5 min at 18,000 × g at 4°C. The precipitates were re-suspended in the suspending buffer and solubilized by 2.0% DDM at 1.0 mg Chl/ml for 2 min on ice. The solubilized samples were centrifuged for 20 min at 18,000×g at 4°C. The supernatant was recovered, and its Chl concentration was determined. Before sample loading, a gel containing a

gradient of 5-12% polyacrylamide was pre-run at a constant current of 4 mA for 1 h at 4°C in a modified cathode buffer of 50 mM Tricine (pH 7.0), 7.5 mM imidazole, 0.05% (w/v) Triton X-100, 0.05% (w/v) deoxycholic acid. After pre-run, the supernatant samples were loaded onto the gel immediately, and electrophoresis was carried out at a constant current of 4 mA.

Gel filtration was performed with a Superdex 200 PC 3.2/30 column equipped to a SMART system (GE Healthcare UK Ltd.) at 10°C [23].

2.3. Measurements of fluorescence emission spectra and oxygen-evolving activity

Fluorescence emission spectra of thylakoid membranes were recorded at 77 K with a fluorescence spectrometer (F-4500, Hitachi) with an excitation wavelength of 435 nm at a Chl concentration of 5 μg/ml.

Oxygen evolution was measured with a Clark-type oxygen electrode under continuous, saturating illumination at 30°C with 0.5 mM phenyl-*p*-benzoquinone and 0.5 mM potassium ferricyanide as electron acceptors, at a Chl concentration of 10 μg Chl/ml. The medium used was 20 mM Mes-NaOH (pH 6.0), 20 mM NaCl, 3 mM $CaCl_2$.

2.4. Crystallization and crystal structure analysis

The isolated PSII dimers were finally concentrated and suspended in a stock buffer containing 25% (w/v) glycerol, 20 mM Mes-NaOH (pH6.0), 20 mM NaCl, 3 mM $CaCl_2$. Crystallization was performed with the hanging drop vapor diffusion method, in which 9 μl sample solutions were vapor-diffused against a reservoir solution of 0.5 ml. For PSII from the ΔYcf12 mutant, the sample solutions contained 2.0 mg Chl/ml, 20 mM Mes-NaOH (pH5.9), 20 mM NaCl, 10 mM $CaCl_2$, 12.5% glycerol, 0.02% DDM, 3.0%-4.0% PEG1,450, and the reservoir solution contained 20 mM Mes-NaOH (pH5.9), 20 mM NaCl, 10 mM $CaCl_2$, 12.5% glycerol, 0.02% DDM, 5.0% PEG1,450. The crystals were grown to a size of 500 μm within 3-4 days at 20°C. For the ΔPsbZ mutant, the pH of the Mes buffer in the sample and reservoir solutions was changed to 6.50.

For X-ray diffraction experiments, PSII crystals were transferred to a cryoprotectant solution containing 25% glycerol and 20% PEG1,450 with a step-wise procedure, and flash-cooled in a nitrogen gas stream at 100 K. The frozen crystals were stored in liquid nitrogen. X-ray diffraction data were collected at beamline BL41XU of a synchrotron radiation facility, Spring-8, Japan [24]. The diffraction patterns were recorded with a

CCD detector Mar225 at an X-ray wavelength of 0.9 Å, an oscillation angle of 0.6°, and an exposure time of 2 sec. The data collected was processed with *HKL2000* [25]. Difference-Fourier maps were calculated with *FFT* in the CCP4 program suit [26].

3. Results

3.1. Characterization of PSII complexes purified from the two mutants

PSII dimers were purified from both ΔYcf12 and ΔPsbZ mutants with the two-steps chromatography in which, the first step used a weak anion-exchange column DEAE 650M and the second step used a strong anion-exchange Q-sepharsoe High Performance column, from crude PSII obtained by LDAO solubilization of thylakoids. Fig. 1 compares gel filtration pattern of the PSII dimers purified from the wild type, ΔYcf12, and ΔPsbZ mutant strains. The PSII dimer preparations from the two mutants had a single peak at a similar position as that of PSII dimers from the wild type strain, indicating that the PSII dimers obtained from the two mutants are homogenous in terms of their sizes.

The polypeptide compositions of PSII complexes from wild type, ΔYcf12 and ΔPsbZ were examined by SDS-PAGE (Fig.2). While most of the PSII components are the same between wild type and mutants, differences were found in the low molecular weight region. In PSII dimers from the wild type strain, a faint band was identified to correspond to Ycf12 by mass spectrometry (data not shown), which was marked Ycf12 in Fig. 2. This band was missing in the ΔYcf12 strain, indicating the deletion of this subunit in the mutant. On the other hand, PSII complexes from the ΔPsbZ mutant still retained a band in the same position after the first column purification, whereas PSII dimers purified by the second column lost this band. Since it has been reported that the final purified PSII from the ΔPsbZ mutant lost Ycf12 [9], the present results suggested that Ycf12 was still associated with PSII in thylakoids of the ΔPsbZ strain and also with PSII after the first weak anion-exchange column, but was lost by the second strong anion-exchange column purification. In contrast, the band of PsbK was lost in both PSII complexes after the first and second column purification in the ΔPsbZ mutant, in agreement with Iwai et al. [9] who reported that deletion of PsbZ destabilizes the binding of PsbK to PSII. In contrast, the band of PsbK was present in PSII dimers from both wild type and ΔYcf12 strains, indicating that deletion of Ycf12 did not affect its binding to PSII.

Table 1 shows the oxygen-evolving activity of thylakoids and purified PSII dimers

from the two mutants in comparison with those from the wild type strain. We constantly observed that the activity of thylakoids from both mutants were lower than that from the wild type. This difference became more evident in the purified PSII dimers, with the activity of PSII from the ΔPsbZ mutant lower than that from the ΔYcf12 mutant. The deviations of oxygen-evolving activities of PSII dimers purified from the ΔPsbZ mutant were also large compared to those of the wild type or ΔYcf12 mutant. This may reflect the fact that PSII from the ΔPsbZ mutant is rather unstable, resulting in the large deviations of the activity of PSII obtained by the prolonged purification procedures.

3.2. Relative content of PSII and PSI in the two mutants in comparison with that in the wild type

In order to investigate whether lower activity affected the stability of PSII in the mutant cells, we measured 77 K fluorescence emission spectra of thylakoid membranes from the wild-type and two mutants. As shown in Fig. 3A, when the fluorescence yield was normalized on the basis of PSI fluorescence at 730 nm (since the two subunits are PSII components, it can be assumed that deletion of either of them should not bring a significant effect on PSI), the amplitude of fluorescence emission from PSII at 685 and 695 nm was lower in the ΔYcf12 strain than that in the wild type strain, and this decrease was more significant in the ΔPsbZ strain. This suggests that the relative content of PSII in the two mutants were decreased than that in the wild type strain, suggesting that PSII was destabilized in the two mutants.

In order to confirm the above results, we analyzed PSII dimers and monomers in the thylakoids of the two mutants in comparison with that from the wild type by hrCNE (Fig. 3B). Pigment-protein complexes corresponding to PSI trimer, PSII dimer, phycobilisome, PSII monomer, and PSI monomer were resolved by the hrCNE-PAGE in the order of their relative molecular weight. Both PSII dimers and monomers were detected in the two mutants; however, the intensity of the band corresponding to PSII dimers was found to be slightly weaker in the mutants than those in the thylakoids of the wild type (It should be pointed that the band of PSII dimer was overlapped with the band of phycobilisome, which makes an accurate estimation of the PSII dimer content difficult). This is consistent with the fluorescence emission spectra, and suggested that deletion of the two subunits mainly destabilized PSII dimers, leading to a relative decrease in the PSII contents. The amount of PSI monomer seemed to be larger in the two mutants than that in the wild type. However, since the position of PSI monomer appeared higher in the wild type, no apparent differences may be found in the amount of

PSI monomer between wild type and the two mutants.

3.3. Crystallization and crystal structure analysis

Crystals of PSII dimers from both ΔYcf12 and ΔPsbZ mutants were obtained by the hanging drop vapor diffusion method. Crystals of ΔYcf12-PSII could be obtained at a similar condition as that of wild type within 2 to 5 days at 20^{o}C, and the shape of the crystals obtained was also similar to those of the wild type crystals (Fig. 4A). Crystals of ΔPsbZ-PSII, however, had to be grown at a higher pH of 6.5, and the shape of the crystals was more irregular than that of the wild type [23] or ΔYcf12 mutant (Fig. 4B).

X-ray diffraction data were collected from crystals of both mutants. The crystallographic data were processed to resolutions of 6.6 Å and 4.7 Å, respectively, from two crystals of the ΔYcf12 mutant PSII, and to a resolution of 6.0 Å from the ΔPsbZ mutant PSII (Table 2). The diffraction data collected from a wild type PSII crystal that had a reasonably good isomorphism with the ΔYcf12 crystals were also shown in Table 2. These results showed that the ΔYcf12 mutant PSII crystals had the same space group $P2_12_12_1$, and similar unit cell dimensions as those of the wild type PSII crystal. The ΔPsbZ mutant PSII crystals had also the same space group of $P2_12_12_1$, but had different unit cell dimensions compared with those of the wild type and ΔYcf12 crystals (Table 2). The volume of the unit cell, however, was similar among all of the crystals from wild type, ΔYcf12, and ΔPsbZ mutants. This suggests that the arrangement of the four PSII dimers within the unit cell of ΔPsbZ has been changed from the wild type or ΔYcf12-PSII crystals.

Difference-Fourier map after non-crystallographic symmetry (NCS) averaging between the wild type and ΔYcf12 mutant PSII crystals was calculated and depicted in Fig. 5. Since the 6.6 Å data set of the ΔYcf12 mutant crystal had a higher isomorphism with that of the wild type crystal (the R_{iso} value between the wild type and the 6.6 Å data set is 0.26, and that between the wild type and the 4.7 Å data set is 0.36), we used this data set to calculate the difference-Fourier map (the 4.7 Å data set gave rise to similar results but with somewhat larger noise signals). As shown in Fig. 5, there was a region with strongly positive signals in the difference-Fourier map, indicating that this region of the electron density was present in the wild type but absent in the ΔYcf12 mutant crystals. This region overlapped with a transmembrane helix closely associated with PsbJ and PsbK in the periphery of PSII dimer. Thus, this helix was identified to correspond to Ycf12. This helix has been designated X1 in the structure of *T. elongatus* reported at 3.0 Å resolution [3], and assigned to Ycf12 in the recent structure reported at

2.9 Å resolution [5]. In the difference-Fourier map, there were no other large signals found, indicating that no significant structural changes had occurred in the ΔYcf12 mutant.

4. DISCUSSION

The present study demonstrated that Ycf12 is located in the periphery of the cyanobacterial PSII dimer adjacent to PsbJ and PsbK, which corresponded to the unassigned helix X-1 in the structure reported at 3.0 Å resolution from *T. elongatus* [3]. This assignment is in agreement with the recent structure at 2.9 Å resolution [5]. In addition to the disappearance of the electron density corresponding to the helix of Ycf12, no significant differences were found in the difference-Fourier map between the wild type and the ΔYcf12 mutant crystals, indicating that no loss of any other subunits occurred in the mutant. This is in agreement with the results from SDS-PAGE analysis. We should point out, however, that some structural changes may have occurred in the mutant PSII which was not detected here due to an insufficient isomorphism between the wild type and mutant crystals, and/or limited resolution.

In contrast to the ΔYcf12 mutant, both Ycf12 and PsbK were found to be lost in purified PSII from the ΔPsbZ mutant, as has been reported previously [9]. This can be explained from the structural point of view, since PsbZ is located in the outmost side of PSII and constitute a cap on Ycf12 and PsbK. Although PsbK has a direct contact with CP43 [27] and Ycf12 is close to PsbK and PsbJ, the loss of PsbZ exposed these two subunits to the surface of the complex, and thus made them labile to dissociation from the complex during detergent solubilization and column purification. In line with this, Ycf12 was still found in PSII after the first, weak anion-exchange column purification, but was lost after the second, strong anion-exchange column purification. These results indicate that Ycf12 was able to bind to PSII weakly in the cells and thylakoid membranes, but its binding affinity to PSII was significantly impaired in the absence of PsbZ. These results also suggest that in the assembly process of PSII, Ycf12 and PsbK are incorporated into the complex before PsbZ is attached. In other words, these subunits are assembled into PSII in the order of Ycf12, PsbK→PsbZ.

The crystals obtained from the ΔPsbZ mutant was found to have a different unit cell dimensions compared with those of wild type and the ΔYcf12 mutant, although the unit cell volume was not different from those of the wild type and the ΔYcf12 mutant. For this reason, the crystallization conditions have to be changed slightly from those used for the wild type and ΔYcf12 mutant. The reason for this change in the unit cell

dimensions can be explained by the molecular contact between adjacent PSII dimers within the unit cell. As shown in Fig. 6, PsbZ in one PSII dimer is located closely to the PsbO subunit from the adjacent dimer; these two subunits may therefore provide a contact for the formation of the crystal lattice. Indeed, a detailed examination showed that the closest distance between the side chain oxygen atom of PsbO-Ser115 in one dimer and the main chain oxygen atom of PsbZ-Phe60 in another dimer is 2.7 Å [5], suggesting that these two atoms may form a hydrogen bond that contributes to the formation and stabilization of the crystal lattice. Loss of PsbZ will break this interaction, and thus changes the arrangement of PSII dimers within the unit cell, leading to the changes in the unit cell dimensions in the mutant. It is interesting to note that, this interaction is formed between a membrane-spanning subunit located in the periphery of one molecule, and a hydrophilic subunit in the adjacent molecule, suggesting that this kind of interaction could be important for the formation of membrane protein crystals. On the other hand, the unit cell dimensions of the ΔYcf12 mutant crystals were the same as those of the wild type strain; this again suggests that deletion of Ycf12 did not affect the binding of PsbZ to PSII, in agreement with the above results. Since PsbZ forms a cap over Ycf12 (and PsbK) as stated above, the binding of PsbZ to PSII in the absence of Ycf12 indicates that PsbZ is associated with PSII mainly through other subunits (most probably PsbK), instead of Ycf12. In this respect, it would be interesting to see whether PsbZ is able to bind to PSII in the absence of PsbK.

The content of PSII dimer was found to be slightly lower in both ΔYcf12 and ΔPsbZ mutants than that in the wild type strain. The oxygen-evolving activity of purified PSII was also decreased in both mutants. These results suggested that deletion of either Ycf12 or PsbZ affected the PSII function, leading to the instability of the PSII complex in vivo. This may account for the previous results that loss of PsbZ affected the association of LHCII with PSII in green alga and higher plants [13, 16]. Alternatively, since PsbZ is located in the outmost side of PSII, it may serve as a direct partner for the binding of LHCII to PSII. The loss of PsbZ may therefore break the association of LHCII with PSII, leading to the dissociation of LHCII from PSII as observed in the previous studies [13, 16]. Since cyanobacterial PSII contains no trans-membrane LHCII, no such phenomenon was observed in the cyanobacterial mutant.

Acknowledgements

This work was supported by a Grant-in-Aid for Scientific Research on Priority Areas (Structures of Biological Macromolecular Assemblies), a Grant-in-Aid for Creative

Scientific Research, a GCOE program on Pico-biology, a Grant-in-Aid for Scientific Research (C), and a Grant-in-Aid for Young Scientists (B) (17770042), from the Ministry of Education, Culture, Sports, Science and Technology of Japan.

REFERENCES

[1] A. Zouni, H.T. Witt, J. Kern, P. Fromme, N. Krauss, W. Saenger, P. Orth, Crystal structure of photosystem II from *Synechococcus elongatus* at 3.8 Å resolution, Nature 409 (2001) 739–743.

[2] K. N. Ferreira, T. M. Iverson, K. Maghlaoui, J. Barber, S. Iwata, Architecture of the photosynthetic oxygen-evolving center, Science 303 (2004) 1831-1838.

[3] B. Loll, J. Kern, W. Saenger, A. Zouni, J. Biesiadka, Towards complete cofactor arrangement in the 3.0 Å resolution structure of photosystem II, Nature 438 (2005) 1040-1044.

[4] N. Kamiya, J.-R. Shen, Crystal structure of oxygen-evolving photosystem II from *Thermosynechococcus vulcanus* at 3.7-Å resolution, Proc. Natl. Acad. Sci. USA 100 (2003) 98-103.

[5] A. Guskov, J. Kern, A. Gabdulkhakov, M. Broser, A. Zouni, W. Saenger, Cyanobacterial photosystem II at 2.9 Å resolution and role of quinones, lipids, channels and chloride, Nat. Struct. Mol. Biol. 16 (2009) 334-342.

[6] K. Kawakami. M. Iwai, M. Ikeuchi, N. Kamiya, J.-R. Shen, Location of PsbY in oxygen-evolving photosystem II revealed by mutagenesis and X-ray crystallography, FEBS Lett. 581 (2007) 4983-4987.

[7] Y. Kashino, T. Takahashi, N. Inoue-Kashino, A. Ban, Y. Ikeda, K. Satoh, M. Sugiura, Ycf12 is a core subunit in the photosystem II complex, Biochim. Biophys. Acta 1767 (2007) 1269-1275.

[8] N. Inoue-Kashino, T. Takahashi, A. Ban, M. Sugiura, Y. Takahashi, K. Satoh, Y. Kashino, Evidence for a stable association of Psb30 (Ycf12) with photosystem II core complex in the cyanobacterium *Synechocystis* sp. PCC 6803, Photosynth. Res. 98 (2008) 323-335.

[9] M. Iwai, T. Suzuki, N. Dohmae, Y. Inoue, M. Ikeuchi, Absence of the PsbZ subunit prevents association of PsbK and Ycf12 with the PSII complex in the thermophilic cyanobacterium *Thermosynechococcus elongatus* BP-1, Plant Cell Physiol. 48 (2007) 1758-1763.

[10] V. V. Goremykin, K. I. Hirsch-Ernst, S. Wolfl, F. H. Hellwig, Analysis of the *Amborella trichopoda* chloroplast genome sequence suggests that amborella is not a basal angiosperm, Mol. Biol. Evol. 20 (2003) 1499-1505.

[11] Y. Kashino, W. M. Lauber, J. A. Carroll, Q. Wang, J. Whitmarsh, K. Satoh, H. B. Pakrasi, Proteomic analysis of a highly active photosystem II preparation from the cyanobacterium *Synechocystis* sp. PCC 6803 reveals the presence of novel

polypeptides, Biochemistry 41 (2002) 8004-8012.

[12] Y. Kashino, H. Koike, M. Yoshio, H. Egashira, M. Ikeuchi, H. B. Pakrasi, K. Satoh, Low-molecular-mass polypeptide components of a photosystem II preparation from the thermophilic cyanobacterium *Thermosynechococcus vulcanus*, Plant Cell Physiol. 43 (2002) 1366-1373.

[13] M. Swiatek, R. Kuras, A. Sokolenko, D. Higgs, J. Olive, G. Cinque, B. Müller, L. A. Eichacker, D. B. Stern, R. Bassi, R. G. Herrmann, F. A. Wollman, The chloroplast gene *ycf9* encodes a photosystem II (PSII) core subunit, PsbZ, that participates in PSII supramolecular architecture, Plant Cell 13 (2001) 1347-1367.

[14] C. L. Bishop, S. Ulas, E. Baena-Gonzalez, E. M. Aro, S. Purton, J. H. Nugent, P. Mäenpää, The PsbZ subunit of Photosystem II in *Synechocystis* sp. PCC 6803 modulates electron flow through the photosynthetic electron transfer chain, Photosynth. Res. 93 (2007) 139-147.

[15] E. Baena-Gonzalez, J.C Gray, E. Tyystjarvi, E. M. Aro, P. Mäenpää, Abnormal regulation of photosynthetic electron transport in a chloroplast *ycf9* inactivation mutant, J. Biol. Chem. 276 (2001) 20795-20802.

[16] S. Ruf. K. Biehler, R. Bock, A small chloroplast-encoded protein as a novel architectural component of the light-harvesting antenna, J. Cell Biol. 149 (2000) 369-378.

[17] M. Iwai, H. Katoh, M. Katayama, M. Ikeuchi, PSII-Tc protein plays an important role in dimerization of photosystem II, Plant Cell Physiol. 45 (2004) 171-175.

[18] J.-R. Shen, M. Ikeuchi, Y. Inoue, Stoichiometric association of extrinsic cytochrome *c*-550 and 12 kDa protein with a highly purified oxygen-evolving photosystem II core complex from *Synechococcus vulcanus*, FEBS Lett. 301 (1992) 145-149.

[19] J.-R. Shen, Y. Inoue, Binding and functional properties of two new extrinsic components, cytochrome *c*-550 and a 12 kDa protein, in cyanobacterial photosystem II, Biochemistry 32 (1993) 1825-1832.

[20] M. Ikeuchi, Y. Inoue, A new 4.8-kDa polypeptide intrinsic to the PSII reaction center, as revealed by modified SDS-PAGE with improved resolution of low-molecular-weight proteins, Plant Cell Physiol. 29 (1988) 1233-1239.

[21] I. Wittig, M. Karas, H. Schägger, High resolution clear native electrophoresis for in-gel functional assays and fluorescence studies of membrane protein complexes, Mol. Cell. Proteomics. 6 (2007) 1215-1225.

[22] H. Schägger, W.A. Cramer, G. von Jagow, Analysis of molecular masses and oligomeric states of protein complexes by blue native electrophoresis and

[23] J.-R. Shen, N. Kamiya, Crystallization and the crystal properties of the oxygen-evolving photosystem II from *Synechococcus vulcanus*, Biochemistry 39 (2000) 14739-14744.

[24] M. Kawamoto, Y. Kawano, N. Kamiya, The bio-crystallography beamline (BL41XU) at SPring-8, Nucl. Instr. Methods A 467-468 (2001) 1375-1379.

[25] Z. Otwinowski, M. Minor, Processing of X-ray diffraction data collected in oscillation mode, Methods in Enzymology 276 part A (1997) 307-326.

[26] Collaborative Computational Project No 4, The *CCP*4 suite: programs for protein crystallography, Acta Crystallogr. D50 (1994) 760-763.

[27] I. Sugimoto, Y. Takahashi, Evidence that the PsbK polypeptide is associated with the photosystem II core antenna complex CP43, J. Biol. Chem. 278 (2003) 45004– 45010.

Table 1

Oxygen-evolving activities of thylakoid membranes and purified PSII dimers from wild-type, Ycf12-deletion mutant, and PsbZ-deletion mutant of *T. elongatus* (μmoles O_2/mg chl/hr).

Strains	Native	ΔYcf12-1	ΔPsbZ
Thylakoid membranes	250-300	160-230	180-250
PSII dimers	3500-4000	2000-2800	1000-2400

Table 2

X-ray diffraction data of PSII crystals collected from wild-type, Ycf12-deletion mutant, and PsbZ-deletion mutant of *T. elongatus*.

Strains	Wild-type	ΔYcf12-1	ΔYcf12-2	ΔPsbZ
X-ray source	BL41XU	BL41XU	BL41XU	BL41XU
Wavelength (Å)	0.9	0.9	0.9	0.9
Resolution (Å)	50-3.90 (4.04-3.90)[a]	50-6.6 (6.84-6.60)[a]	50-4.7 (4.87-4.70)[a]	50-6.0 (6.21-6.00)[a]
Observed reflections	606,760	109,254	311,127	171,389
Unique reflections	82061	16,770	43,202	23,512
Rmerge (%)	8.6(77.9)[a]	9.9(70.3)[a]	8.8(87.0)[a]	12.0(71.1)[a]
I/σ(I)	24.3(2.3)[a]	18.8(1.9)[a]	28.0(2.3)[a]	18.2(2.0)[a]
Redundancy	7.4(7.5)[a]	6.5(6.7)[a]	7.2(7.4)[a]	7.3(7.5)[a]
Completeness	99.9(100)[a]	98.0(100)[a]	95.3(99.4)[a]	99.0 (100)[a]
Space group	$P2_12_12_1$	$P2_12_12_1$	$P2_12_12_1$	$P2_12_12_1$
Unit cell dimensions (Å)				
a	128.7	130.0	129.4	154.5
b	225.8	224.3	225.2	224.5
c	305.6	304.3	302.3	259.2
Unit cell volume (x 10^6 Å^3)	8.88	8.87	8.81	8.99

[a]Numbers in parentheses represent the highest-resolution shell.

Figure legends

Figure 1. Gel filtration elution patterns of PSII dimers with a column Superdex 200 HR 30/10.
(A) Solid line, PSII dimers from the Ycf12-deletion mutant; dashed line, PSII dimers from wild-type. (B) Solid line, PSII dimers from the PsbZ-deletion mutant; dashed line, PSII dimers from the wild-type.

Figure 2. SDS-PAGE analysis of PSII dimers from the wild type and two mutans.
Lane 1, wild type PSII dimers; lane 2, PSII dimers from the ΔYcf12 mutant; lane 3, PSII complexes purified from the the ΔPsbZ mutant after the first column; and lane 4, PSII dimers purified after the second column from the ΔPsbZ mutant. The amount of PSII loaded was 5 μg Chl for each lane.

Figure 3. Analysis of PSII dimers and monomers in the thylakoid membranes by low temperature fluorescence emission and high resolution clear native PAGE (hrCNE).
(A) Fluorescence emission spectra at 77 K from thylakoid membranes of wild type and the two mutants. Thylakoid membranes were excited at a wavelength of 435 nm at 5 μg Chl/ml, and the fluorescence amplitudes were normalized by the intensity at 730 nm. Four independent samples were measured for the wild type and each of the mutants, and the spectra obtained were averaged. Black, wild-type; red, ΔYcf12 mutant; blue, ΔPsbZ mutant. (B) High resolution clear native PAGE (hrCNE) analysis of the thylakoids from the wild type, ΔYcf12 and ΔPsbZ mutants. Lane 1, wild type; lane 2, ΔYcf12 mutant; lane 3, ΔPsbZ mutant. The amount of thylakoids loaded was 15 μg Chl per lane.

Figure 4. Crystals of PSII dimers from the two mutants.
(A) Crystals of PSII dimers from the ΔYcf12 mutant grown at 20^{o}C for 4-5 days. (B) Crystal of PSII dimers from the ΔPsbZ mutant grown at 20^{o}C for 6-7 days. See text for more detailed crystallization conditions.

Figure 5. Difference-Fourier map of wild-type-minus-ΔYcf12 mutant PSII.
(A) Difference-Fourier map of wild-type-minus-ΔYcf12 mutant PSII superimposed

with the structure of PSII at 2.9 Å [5]. Only the PSII monomer structure was shown. Top view from the lumenal side. (B) Same as in (A), with a view from the side of the membrane plane. Blue mesh, positive signals; violet mesh, negative signals

Figure 6. Arrangement of PSII dimers within a unit cell of the crystal lattice.
(A) Arrangement of four dimers within the unit cell. The structural model of PSII at 2.9 Å resolution from *T. elongatus* [5] was shown. Color codes: Orange, PsbO; blue, PsbZ; green, other subunits of PSII. (B) An enlargement view of the region joining two dimers within the unit cell. Color codes are the same as in (A).

Fig. 1

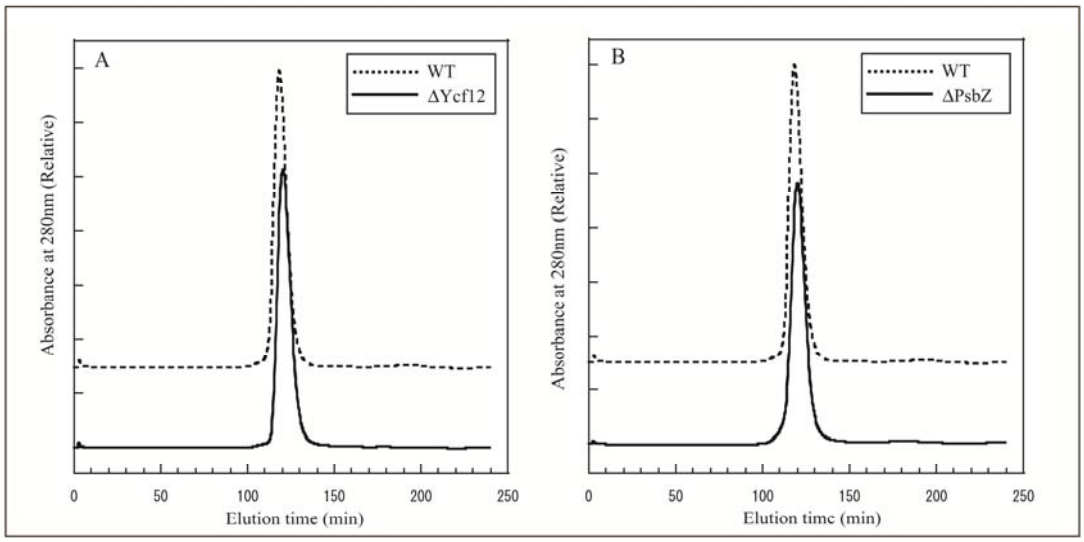
A
WT
ΔYcf12
Absorbance at 280nm (Relative)
0
50
100
150
200
250
Elution time (min)
B
WT
ΔPsbZ
Absorbance at 280nm (Relative)
0
50
100
150
200
250
Elution time (min)

Fig. 2

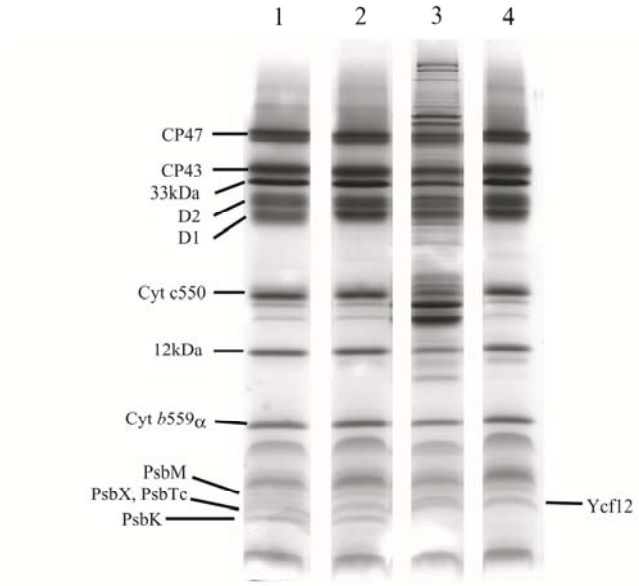
1
2
3
4
CP47
CP43
33kDa
D2
D1
Cyt c550
12kDa
Cyt b559α
PsbM
PsbX, PsbTc
PsbK
Ycf12

Fig. 3

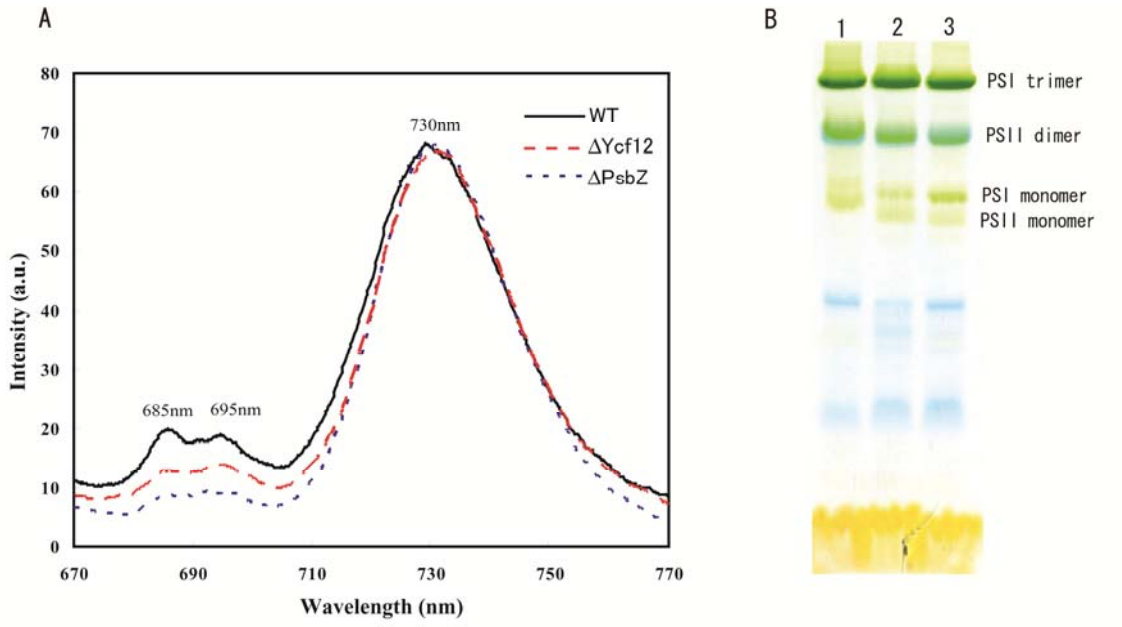
A
B
1
2
3
PSI trimer
PSII dimer
PSI monomer
PSII monomer
WT
ΔYcf12
ΔPsbZ
730nm
685nm
695nm
Intensity (a.u.)
Wavelength (nm)
0
10
20
30
40
50
60
70
80
670
690
710
730
750
770

Fig. 4

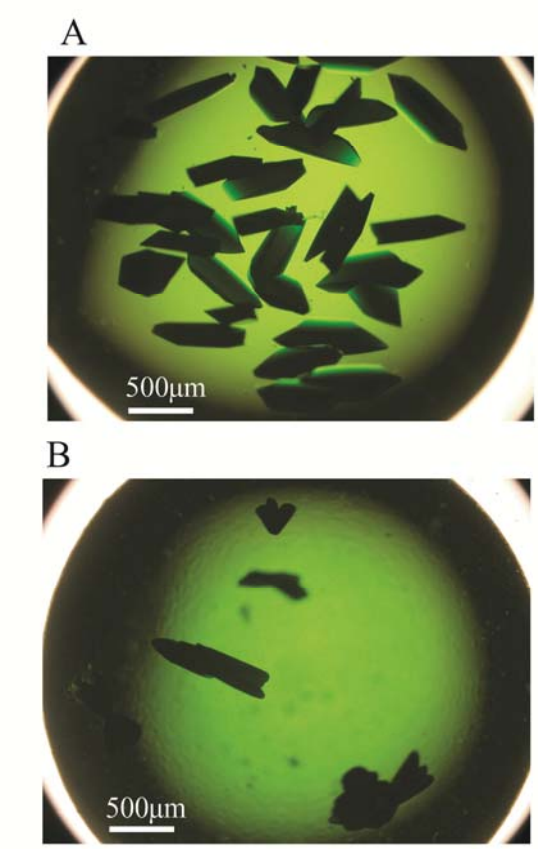
A
500μm
B
500μm

Fig .5

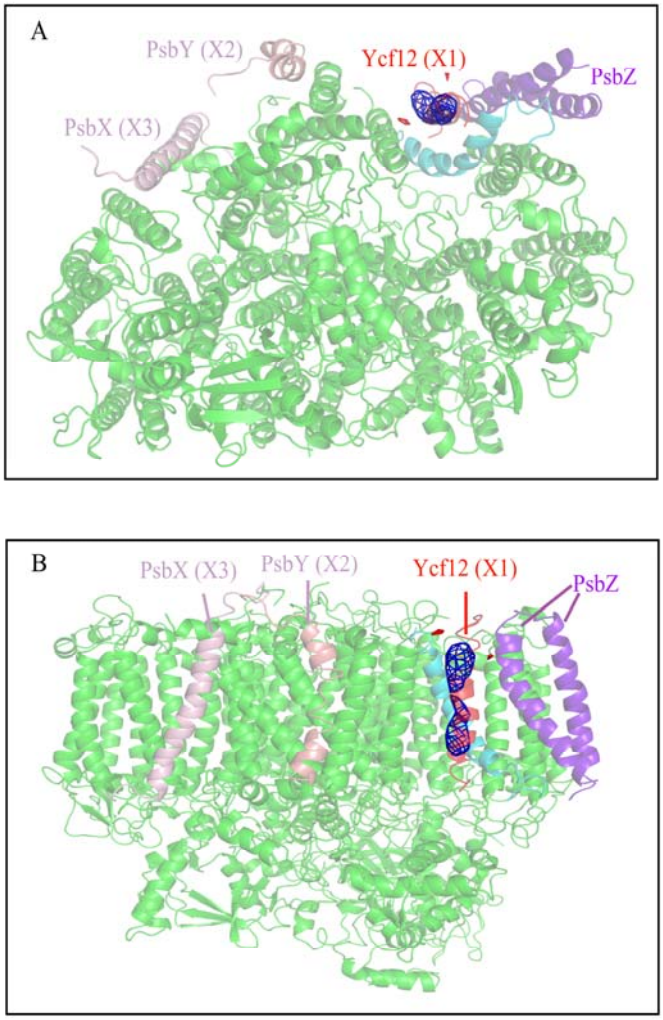
A
PsbY (X2)
Ycf12 (X1)
PsbZ
PsbX (X3)
B
PsbX (X3)
PsbY (X2)
Ycf12 (X1)
PsbZ

Fig. 6

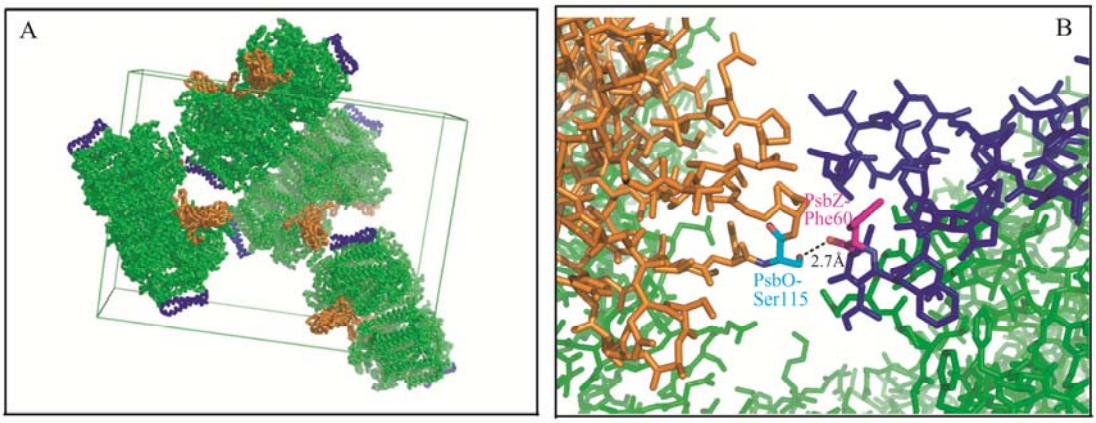
A
B
PsbZ-
Phe60
2.7Å
PsbO-
Ser115